



Published in final edited form as:

Nat Rev Clin Oncol. 2014 November ; 11(11): 670–680. doi:10.1038/nrclinonc.2014.134.

Quantitative multimodality imaging in cancer research and therapy

Thomas E. Yankeelov, Richard G. Abramson, and C. Chad Quarles

Department of Radiology and Radiological Sciences, Vanderbilt University Institute of Imaging Science, Vanderbilt University Medical Center, AA-1105 Medical Center North, 1161 21st Avenue South, Nashville, TN 37232-2310, USA (T.E.Y., R.G.A., C.C.Q.)

Abstract

Advances in hardware and software have enabled the realization of clinically feasible, quantitative multimodality imaging of tissue pathophysiology. Earlier efforts relating to multimodality imaging of cancer have focused on the integration of anatomical and functional characteristics, such as PET–CT and single-photon emission CT (SPECT–CT), whereas more-recent advances and applications have involved the integration of multiple quantitative, functional measurements (for example, multiple PET tracers, varied MRI contrast mechanisms, and PET–MRI), thereby providing a more-comprehensive characterization of the tumour phenotype. The enormous amount of complementary quantitative data generated by such studies is beginning to offer unique insights into opportunities to optimize care for individual patients. Although important technical optimization and improved biological interpretation of multimodality imaging findings are needed, this approach can already be applied informatively in clinical trials of cancer therapeutics using existing tools. These concepts are discussed herein.

Introduction

The requirement to study cancer *in vivo* for diagnostic, therapeutic, and prognostic purposes has encouraged the development of imaging technologies that can interrogate the anatomical, functional, and molecular characteristics of both primary and meta-static disease in a noninvasive and quantitative way (Box 1). Because cancer is such a complex phenomenon, no single imaging modality can answer all the questions of interest; however, many imaging techniques are complementary in nature, and combining their strengths in multimodality imaging studies has the potential to provide a more-complete characterization of tumours and their environment. Initial efforts in multimodality imaging were designed to improve the accuracy of interpretation of study results by associating functional and anatomical data; in particular, the functional data provided by the nuclear methods of single-photon emission CT (SPECT–CT) and PET were integrated with the anatomical data

Correspondence to: T.E.Y. thomas.yankeelov@vanderbilt.edu.

Competing interests

T.E.Y. has been a consultant for Eli Lilly.

R.G.A. and C.C.Q. declare no competing interests.

Author contributions

All authors contributed substantially to all stages of the preparation of the manuscript for submission.

provided by X-ray CT. These efforts have proven enormously successful, and have provided critical motivation for synthesizing other types of imaging data. Logically, the next step in the evolution of multimodality imaging will involve integrating quantitative information from multiple existing functional and/or molecular modalities into composite datasets. Although dramatic advances in imaging technology have made such opportunities a reality, fundamental barriers need to be overcome before we see new combined imaging techniques deployed routinely in the clinical setting.

Box 1

Definitions of types of imaging assessments

Finding widely agreed upon and accepted definitions of the various important purposes of noninvasive imaging modalities, such as CT, MRI, and PET, is difficult. In this manuscript, we adopt the following definitions of the key uses of imaging in the clinical setting:

- Anatomical imaging: techniques that reveal the morphology of individual structures of the body and their geometric relationships
- Quantitative imaging: modalities that provide measurements of intrinsic tissue properties (including anatomical, physiological, or biophysical parameters) specified in appropriate continuous-variable units⁷¹
- Molecular imaging: approaches that report on the spatiotemporal distribution of molecular or cellular processes for biochemical, biological, diagnostic, or therapeutic applications⁷²
- Functional imaging: any technique that provides data beyond anatomical information; a general term encompassing both quantitative and molecular imaging techniques that provide information on the activity of biological processes

Standard-of-care medical imaging is capable of depicting human anatomy in exquisite detail. For example, CT and MRI can rapidly acquire images with extraordinary spatial resolution and tissue contrast, whereas older modalities, including standard radiography and mammography, have been transformed into digital technologies that offer superior diagnostic accuracy compared with the electronic analogue methods used routinely just a few years ago.¹ Medical images can now be optimized to separate and quantify the multiple complicated biological and physical phenomena contributing to measured tissue contrast; for example, techniques are currently available for reporting on tissue blood flow (Box 2), cellularity, or metabolism using continuous-variable numerical units. Quantitative multimodality imaging approaches are motivated by the hypothesis that combining these advanced techniques will result in data that are intrinsically more sensitive to the underlying cancer biology (that ultimately determines tumour type and grade, and, therefore, treatment planning) than the morphological features available in routine radiological imaging.

Box 2**Multimodality imaging and vascular normalization**

The normalization of abnormal—overdilated, tortuous, disrupted, and hyperpermeable—tumour blood vessels following antiangiogenic therapy is an emerging strategy that has shown potential over the past decade. Critical to the successful clinical implementation of this approach is the reliable determination of the ‘vascular normalization window’ (that is, the time during which perfusion and oxygen delivery in the tumour becomes more efficient⁷³) to guide the use and, therefore, maximize the therapeutic efficacy of secondary therapies (chemotherapy, and/or radiotherapy, and/or targeted agents). Currently, inpatient and outpatient temporal variation in the vascular normalization window is poorly characterized. Nevertheless, multifunctional imaging has shown promise in detecting the normalization of abnormal tumour vessels after the administration of antiangiogenic therapy. Specifically, in a series of studies evaluating the pan-VEGFR tyrosine kinase inhibitor, cediranib (also known as AZD2171),^{74–77} DCE–MRI, DSC–MRI, and diffusion-weighted MRI were used together with traditional anatomical imaging methods to assess patients with glioblastoma before, during, and after therapy. Imaging parameters, specifically vascular permeability and vessel-size estimates from DCE–MRI and DSC–MRI data, respectively, were combined with circulating levels of type IV collagen to define a ‘vascular normalization index’, which was shown to correlate closely with overall and progression-free survival.⁷⁵ Lending further evidence that these effects were related to vascular normalization, patient survival at 6 months after therapy was higher in patients with tumours that exhibited transiently increased perfusion (lasting approximately 1 month) following antiangiogenic therapy;⁷⁶ however, some controversy exists regarding the most-appropriate interpretation of these findings.⁷⁸ Nevertheless, these data provide a compelling rationale for evaluating changes in hypoxia (using FMISO-PET, for example), cellular proliferation (via FLT-PET, for instance), or apoptosis (by ^{99m}Tc-labelled annexin V single-photon emission CT⁷⁹) after radiotherapy and/or chemotherapy administered during the MRI-detected vascular normalization window.

Abbreviations: DCE–MRI, dynamic contrast-enhanced MRI; DSC–MRI, dynamic susceptibility contrast MRI; FLT, 3'-¹⁸F-fluoro-3'-deoxythymidine; FMISO, ¹⁸F-fluoromisonidazole; VEGFR, vascular endothelial growth factor receptor.

This article describes the current status and expected future evolution of quantitative multimodality functional imaging in oncology. We review the important applications of multimodality imaging and present supportive examples from the literature. The practical limitations restricting the adoption of quantitative multimodality methods are also discussed, and barriers such as cost, availability, and reproducibility issues, as well as the general increase in overall complexity of data, are highlighted. In addition, we outline our vision of how quantitative multimodality imaging can contribute to the clinically relevant field of predictive oncological imaging.

Available quantitative data

Beyond the anatomical information provided by standard high-resolution MRI and CT sequences, an enormous amount of functional data can be obtained using the major *in vivo* cross-sectional imaging modalities that are suitable for application in clinical studies. In the following sections we discuss various tumorigenic processes that can be analysed in further detail with such imaging modalities.

Imaging vascular and oxygen status

The most-common physiological imaging measures are based on characterizations of vascular structure, haemodynamics, and oxygen status. These three entities are intimately related to the process of tumour neo-vascularization, which is one of the principal targets for quantitative imaging of tumours. In contrast to mature blood vessels, which are associated with normal tissue, tumour vessels produced by angiogenesis are characteristically leaky, fragile, immature, and disrupted.² Currently, the most-powerful techniques for characterizing tumour neovasculature include dynamic contrast-enhanced MRI (DCE-MRI),³ contrast-enhanced CT,⁴ and microbubble-enhanced sonography⁵ (although, in the USA, no ultrasound contrast agents are currently approved for cancer imaging). These techniques, to varying degrees, can be used to obtain estimates of tumour blood flow, vessel permeability, tissue-volume fractions (that is, how much of a given section of tissue is comprised of different components, such as vascular, extravascular, and cellular space), transit time (the mean time for a contrast agent to pass through a voxel's vascular tree), and extraction fraction (the fraction of contrast agent that enters the extravascular space from the vascular space in one capillary pass). Thus, these methods provide a way of quantifying changes in tumour-associated blood vessels, for example, in response to antiangiogenic drugs.

Oxygen status is intimately related to these vascular parameters. Imaging techniques that can be used to quantify tissue oxygen status include ¹⁸F-fluoromisonidazole PET (FMISO-PET), and ⁶⁴Cu-diacetyl-bis(*N*⁴-methylthiosemicarbazone) PET (Cu-ATSM-PET).^{6,7} In general, after entering a cell, the tracers used in these approaches (FMISO and Cu-ATSM) are reduced and retained in hypoxic conditions, but exit the cell freely under normoxic conditions, which forms the basis for quantitation of oxygen levels.^{6,7} Oxygen status can also be assessed semiquantitatively using an MRI protocol based on the blood-oxygen-level-dependent (BOLD) signal,⁸ which is the foundation of functional MRI of the brain. The BOLD contrast effect relies on the creation of magnetic-susceptibility-induced inhomogeneity in the magnetic fields surrounding blood vessels that contain deoxyhaemoglobin; the transverse relaxation rates of water protons in blood and in the tissue surrounding the blood vessels are enhanced by the presence of deoxyhaemoglobin and, therefore, these relaxation rates vary depending on the local concentration of deoxyhaemoglobin. Thus, such variations in relaxation rates provide a sensitive measure of changes in blood oxygen saturation. Although other MRI methods have been developed that enable more accurate quantitation of tumour oxygen status than BOLD-MRI,⁹ they have not been deployed widely in clinical studies due to the current complexity of the technique.

Cellularity and cell proliferation

By perhaps the most-basic definition, cancer is a disease (or group of diseases) characterized by unregulated cell growth and proliferation, and many anticancer therapies aim to halt these processes, with the ultimate goal of causing tumour-cell death. Accordingly, imaging modalities that are sensitive to changes in the cellularity of tissues are an important requirement in medicine. A range of imaging techniques based on both MRI and PET offer opportunities for analysis of various aspects of tumour cellularity in clinical studies.

The apparent diffusion coefficient (ADC) is a term used to describe the rate of diffusion of water in cellular tissues, and this parameter is heavily dependent on the number, properties, and separation of barriers that a diffusing water molecule encounters. Regional variations in ADC can be mapped within tissues using diffusion-weighted MRI (DW-MRI) protocols, and this variable has been shown to be inversely correlated with tissue cellularity in well-controlled studies.¹⁰ Thus, DW-MRI provides information on tumour density and cellularity, which is particularly important in monitoring response to cytotoxic therapies.

In addition, quantitation of cellular proliferation might be possible using the PET tracer 3'-¹⁸F-fluoro-3'-deoxythymidine (FLT).¹¹ This molecule is an analogue of thymidine, which is an endogenous nucleoside that is taken up by cells via cell-surface nucleoside transporters. Once inside the cell, thymidine is phosphorylated by the enzyme thymidine kinase 1 (TK1), producing thymidine monophosphate. Both TK1 expression and activity are upregulated during the DNA-synthesis phase of the cell cycle, and thymidine is preferentially taken up by rapidly proliferating cancer cells. In an analogous manner, FLT is transported from the blood plasma to the cytosol of cells and is subsequently metabolized to FLT monophosphate. FLT monophosphate can then be modified to produce FLT diphosphate and triphosphate via further sequential phosphorylation events mediated by thymidylate kinase and diphosphate kinase, respectively. FLT triphosphate cannot be stably incorporated into the growing DNA chain as the free hydroxyl group at the 3' position of the ribose moiety of deoxyribonucleotides is substituted by ¹⁸F in FLT in lieu of the endogenous -OH; thus, FLT monophosphate, diphosphate, and triphosphate will accumulate in cells that have high levels and activity of TK1 required for DNA replication (including tumour cells), and this pattern forms the basis of FLT-PET imaging of cell proliferation.

Imaging metabolism

The molecular-imaging tool used most widely in clinical practice is the PET tracer 2-¹⁸F-fluoro-2-deoxy- β -D-glucose (FDG).¹² As a glucose analogue, FDG is taken up by tumour cells (among other cell types) via the glucose transporters type 1 and type 3, and is subsequently phosphorylated by hexokinase to FDG-6-phosphate; however, unlike glucose-6-phosphate, FDG-6-phosphate is not metabolized further in the glycolytic pathway and, therefore, accumulates in tumour cells, which often do not express substantial amount of glucose-6-phosphatase to counteract the activity of hexokinase. The rate of glucose metabolism can differ between healthy and malignant tissues, as well as within particular tissues (for example, tumours) in response to therapy, which is reflected by variations in the rate of FDG uptake, metabolism, and accumulation (Figure 1a). The capacity of FDG-PET to characterize such variations in metabolic activity is the reason why FDG-PET is frequently

selected for application in clinical studies; in fact, the most-recent version of the Response Evaluation Criteria In Solid Tumors (RECIST)¹³ includes the use of FDG-PET for assessing progressive disease in certain situations. This recommendation represents the first time a nonanatomical imaging method has been included in widely accepted guidelines for assessing tumour response.

Imaging receptor status

A number of PET tracers that target various cellular receptors are also available. For example, ¹⁸F-fluoroestradiol (FES) is an oestrogen receptor (ER)-specific PET tracer that is appropriate for application in assessments of the ER status of tumours and localization of ER-positive breast cancers.¹⁴ Radiotracers also exist for PET imaging of progesterone receptor (PR), HER2, and EGFR expression.¹⁵ These tracers can be used not only for tumour localization and treatment selection, but also for predicting response to targeted therapies. An example of molecular imaging of cell-surface receptors in general is provided by PET with radiolabelled choline as the tracer. As the rate of cell-membrane synthesis is increased in many tumours (as a result of increased cell growth), elevated uptake of ¹⁸F-fluorocholine or ¹¹C-choline is frequently observed.¹⁶

Potential applications

The initial driving motivation for the development of multimodality imaging approaches was the need for more-precise anatomical localization of structures than was possible by low-spatial-resolution nuclear-medicine tomographic scans. As early as the mid-1960s, investigators were experimenting with transmission CT scanning as an adjunct to emission CT (SPECT) for correlating radioisotope deposition with radiographic anatomical information.¹⁷ Subsequently, the contemporary SPECT–CT system was developed in the late 1980s and early 1990s,^{18–20} and a combined PET–CT scanner was introduced in 2000.²¹ Acquiring transmission CT images together with emission scintigraphy enables the ‘fusion’ of data on form and function; specifically, functional imaging data can be overlaid on a high-resolution anatomical map (Figure 1). Furthermore, in this combined approach, attenuation correction of the emission data (that is, the process by which the CT data are used to construct an attenuation map to correct for the absorbance and scattering of the photons emitted from the radionuclide) is possible using the transmission CT data.²² The combined PET–CT strategy has proven so successful that the major manufacturers of medical imaging technologies no longer offer stand-alone PET scanners without an integrated CT scanner; consequently, the standalone PET scanner is rapidly disappearing from the clinical landscape.

The success of modern PET–CT methodologies has contributed to the broad motivation for integration of quantitative multimodality imaging into the clinical arena. Applications of quantitative multimodality imaging in cancer have coalesced around three clinically and biologically relevant objectives, which are discussed in the following sections: first, improving the ability to diagnose and stage disease; second, improving the ability to assess and predict treatment response; and third, providing *in vivo* insights into cancer biology.

Improving diagnosis and staging

PET–CT—PET–CT is used widely for a variety of indications in oncology, including diagnosis, staging, and restaging of lung, colorectal, oesophageal, breast, and head and neck cancers, as well as lymphoma.²³ Head-to-head comparative investigations have shown PET–CT to be more accurate than PET alone for staging of non-small-cell lung cancer (NSCLC),^{24,25} colorectal cancer,²⁶ head and neck cancers,²⁷ and neuroendocrine tumours.²⁸ Owing to the accrual of complementary data, hybrid PET–CT imaging improves the diagnostic accuracy of standalone PET and CT studies not only by facilitating the localization of scintigraphic lesions, but also for a number of other reasons: by providing data for attenuation correction; improving discrimination between physiological and pathological radiotracer uptake; detecting a greater number of lesions; enhancing differentiation of benign from malignant lesions; providing better delineation of tumour boundaries for biopsies, surgery, and radiotherapy; and improving the assessment of disease activity in the presence of residual morphological abnormalities after therapy.²⁹

PET–MRI—A more-recent advance in multimodality imaging has been the introduction of hybrid PET–MRI scanners.^{30,31} As MRI offers better soft-tissue contrast than CT, PET–MRI is expected to be superior to PET–CT for anatomical localization of PET findings in areas with low inherent CT contrast, such as the neck, the upper abdomen, and the female pelvis.^{32,33} Indeed, preliminary studies comparing PET–MRI and PET–CT have demonstrated higher diagnostic accuracy for PET–MRI in oral squamous-cell carcinoma³⁴ and pancreatic cancer.³⁵ Moreover, in a study that compared the performance of PET–MRI and PET–CT assessments carried out on the same day in 134 patients with various malignancies, discordant findings of potential clinical relevance were reported;³⁶ 24 patients (17.9%) had findings that were noted on PET–MRI but not on PET–CT, compared with two patients (1.5%) who had findings identified with PET–CT that were not detected using PET–MRI.³⁶ In the context of paediatric tumours of the central nervous system (CNS), compared with FDG-PET alone, the coregistration of FDG-PET and MRI anatomical data improved the diagnostic accuracy (malignancy grading) in 28 of 31 patients (increased specificity in 90% of cases as verified by histology), and more precisely defined the tumour location in 23 patients.³⁷ Furthermore, in a study of 119 patients, the fusion of FDG-PET and MRI significantly improved the accuracy of differentiating between benign lesions and malignant pancreatic tumours compared with FDG-PET–CT (96.6% versus 86.6%, $P = 0.005$).³⁸ Such findings indicate the potential diagnostic value of PET–MRI.

Importantly, however, not all of the comparative studies of multimodality imaging performed to date have demonstrated the superiority of this approach over single-modality methods. For example, Pfluger *et al.*³⁹ detected and monitored 813 lesions—originating from multiple anatomical sites—in paediatric patients using PET and MRI in order to determine the diagnostic value of each modality alone and combined; the coregistered PET–MRI images proved to be most valuable for the detection and staging of multifocal disease in individual patients, owing to the complimentary information afforded by each modality. Conversely, FDG-PET alone was superior to MRI alone or PET–MRI when assessing therapeutic response during follow-up examinations (considering pretreatment and post-treatment images).³⁹ This pattern was attributed to difficulties with using MRI to identify

viable bone marrow versus bone marrow lesions at the selected time of scanning.³⁹ Consequently, the diagnostic utility of anatomical and functional image registration might be specific to disease origin and/or the treatment regimen used, warranting further investigation.

Beyond the fusion of anatomical and functional readouts, multiparametric or multifunctional imaging studies offer the ability to combine complementary signatures of cancer in order to better characterize disease status. For example, integrating FDG-PET and DCE-MRI data has been used to overcome the low diagnostic specificity of MRI for breast tumours. Walter *et al.*⁴⁰ demonstrated that MRI achieved a sensitivity and specificity of 89% and 74%, respectively, whereas FDG-PET achieved 63%, and 91%, respectively. When the two methods were combined, the authors claim that the percentage of unneeded biopsies (that is, obtaining a biopsy when the lesion was benign) could be reduced from 55% to 17%.

Multiparametric MRI—One of the assets of MRI is that multi-functional and anatomical studies can be carried out during a single examination, without the need for multiple injections of tracers or moving the patient between imaging systems (Figure 2). As neurological examinations are less prone to artefacts that are encountered in assessments of other tissues (such as cardiac and respiratory motion, and magnetic-susceptibility artefacts), numerous multifunctional MRI studies have been performed in patients with brain cancer. In particular, many studies have sought to determine the ability of MRI protocols, either alone or in combination, to differentiate between high-grade and low-grade brain tumours. For example, Zonari *et al.*⁴¹ used DW-MRI, magnetic resonance spectroscopy (MRS), and dynamic susceptibility contrast MRI (DSC-MRI) to characterize glioma cellularity, biochemistry, and perfusion, respectively, in 105 patients; tumour blood volume was found to be the most-effective parameter for glioma grading (sensitivity and specificity of 81.5% and 70%, respectively).⁴¹ Interestingly, MRS enabled quantitation of the *N*-acetylaspartate-to-creatine (NAA:Cr) ratio—a known neural marker—which was found to be the next most-robust parameter for differentiating low-grade and high-grade tumours, with lower NAA:Cr ratios (indicative of fewer neurons) observed in high-grade tumours. A logistic regression analysis of all the MRI-derived parameters, including normalized cerebral blood volumes, the NAA:Cr ratio, the ADC, the choline-to-creatine (Cho:Cr) ratio, and lactate and lipids levels resulted in an increased sensitivity (90.8%) and specificity (77.5%) of glioma grading. Since this study was published, similar results have been reported in cancers localized outside the brain. For instance, by combining DW-MRI (ADC) and DCE-MRI (time-intensity curve pattern) parameters, benign and malignant parotid tumours were distinguished with greater accuracy (94% versus 82%) and an increased positive predictive value (92% versus 67%) than with DCE-MRI alone.⁴² In patients with prostate cancer, the combination of DW-MRI-derived ADC with a MRS-derived metabolic index—(choline + polyamine + creatine)/citrate—was able to better differentiate benign from malignant peripheral-zone prostatic tissue, compared with MRS ($P = 0.005$) or ADC alone ($P = 0.09$).⁴³ These studies underscore the role of multifunctional imaging for diagnostic and staging purposes, as well as the fact that the diagnostic parameters need to be specifically selected for each tumour type to realize the full potential of multifunctional assessments. In practice, multifunctional MRI studies would probably be most beneficial in cases in which tumour resections (and/or biopsies) are used exclusively for diagnostic, and not therapeutic,

purposes; for example, in the differential diagnosis of gliomas and primary CNS lymphomas.

Correlating imaging and omics data—More recently, studies have incorporated genomic and proteomic assays to gain new insights into how the underlying tissue biology is manifested on clinical images, thereby improving imaging-based diagnostics. Indeed, the fact that genetic and proteomic heterogeneity might be reflected in radiographic features has been hypothesized. In the context of patients with liver cancer, Segal *et al.*⁴⁴ found that a combination of 28 CT-imaging traits was correlated with 78% of the global gene-expression profiles of tumour tissues, in particular those influencing cellular proliferation and liver synthetic function. The authors concluded that conventional clinical imaging data could enable serial molecular profiling of tissues.⁴⁴ In addition, these promising results raise the following question: if anatomical imaging analyses can capture 78% of the genetic variation in tumours, can multifunctional imaging capture the remaining 22%?

To evaluate the prognostic significance of FDG-PET and identify CT imaging features that are highly correlated with genetic features in a cohort of patients with NSCLC, Gevaert *et al.*⁴⁵ took advantage of public genetic databases in which data on gene expression and clinical outcome are readily available. This study reported that approximately 63% of the CT-imaging features (114 out of a total of 180) and the PET standardized uptake value (SUV) could be predicted based on clusters of coexpressed genes (metagenes) with an accuracy of 65–86%.⁴⁵ The imaging features that were most-closely correlated with clinical outcome included the size, edge shape, and margin sharpness of tumours.⁴⁵ Thus, ‘radiogenomics’ has already enabled the identification of new prognostic biomarkers based on conventional anatomical imaging characteristics and holds the potential to provide new insights into their molecular underpinnings.^{44–47} A reasonable hypothesis is that the clinical utility of radiogenomics can only be enhanced by incorporating multifunctional imaging datasets. It should be noted that as the days of whole-genome sequencing for less than US \$1,000 have arrived, such (comparatively expensive) imaging studies must be justified. A second point to consider is whether the gene mutations identified to correlate with imaging features are predominantly driver or passenger in nature. An application in which radiogenomics is of particular interest is in the assessment of disease sites that are difficult to biopsy, or in situations in which repeat biopsies are not practical.

Informing on therapeutic response

Predicting response to therapy—Noninvasive imaging is a mainstay of treatment-response assessment in clinical trials, given practical barriers in performing serial tumour biopsies, including poor patient tolerance and spatial sampling. The RECIST criteria¹³ represent the current standard for imaging-based response assessment in clinical trials involving patients with solid tumours. These guidelines offer a straightforward and practical method for evaluating response based on changes in tumour size over time. However, changes in tumour size can lag weeks behind induction of tumour-cell arrest and/or death, raising doubts about the ability of the RECIST criteria to capture meaningful biological changes at early time points during treatment. Importantly, changes in tumour size might underestimate or fail to capture the antitumour efficacy of newer drugs that might be

predominantly cytostatic, rather than cytotoxic, such as antiangiogenic agents.^{48–50} However, the fact that the RECIST criteria can adequately capture when a therapeutic regimen is failing should be recognized; in such cases the size of the tumour will frequently increase early in the course of therapy. The promise of multimodality functional imaging in the context of treatment-response assessments lies in the presumed ability of this approach to enable characterization of the underlying physiological, cellular, and molecular changes with greater sensitivity and predictive ability than changes in anatomical size.

Jansen and colleagues⁵¹ evaluated whether ¹H-MRS, DCE-MRI, and FDG-PET performed before treatment administration could predict the response of nodal metastases to chemotherapy in 16 patients with head and neck squamous-cell carcinoma (HNSCC). In terms of predicting short-term outcome, a regression analysis revealed that the mean SUV of FDG and the standard deviation of K^{trans} (the volume transfer constant from DCE-MRI) achieved area under the receiver operator characteristic curve (AUC) values of 0.87 and 0.5, respectively. However, when these two measures were combined, the AUC increased to 0.96, providing encouraging preliminary evidence that prediction of therapeutic response can be improved by combining data from two imaging modalities.

In a study that assessed a population of patients with HNSCC using both FDG-PET and FMISO-PET, Thorwarth *et al.*⁵² examined the relationship between the uptake of the two PET tracers before and after treatment with radiotherapy. Although neither parameter alone could reliably stratify patient groups with respect to treatment outcome, the width of the scatter plots (FMISO uptake versus FDG uptake in each tumour) predicted treatment success;⁵² specifically, the width of the scatter plots was more than 30% greater in patients who exhibited poor response to therapy than in patients with a good therapeutic response ($P = 0.008$), indicating that weakly correlated uptake of FDG and FMISO might reflect a more-malignant tumour phenotype.⁵² This finding demonstrates the potential of multifunctional readouts to inform on the biology and intrinsic heterogeneity of tumours—something pathology struggles to capture over the whole tumour volume—in order to predict treatment outcome before its initiation.

Radiotherapy planning—Over a decade ago, the concept of ‘biological target volume’ (BTV) was introduced as a means to improve both target delineation and dose delivery in radiotherapeutic planning, primarily through the incorporation of biological imaging metrics sensitive to relevant pathophysiological, genotypic, and phenotypic tumour features that affect radiosensitivity.⁵³ Vera *et al.*⁵⁴ extended this effort by evaluating the combined use of fully registered FDG-PET, FMISO-PET, and FLT-PET to evaluate changes in glucose metabolism, hypoxia, and cell proliferation, respectively, before and at two time points during radiotherapy in patients with NSCLC. Overall, the uptake of FLT and FDG within tumours decreased rapidly and significantly during radiotherapy (46 Gy), with SUV_{max} values before and during therapy of 4.7 versus 2.2 for FLT ($P = 0.00006$), and 6.1 versus 4.3 for FDG ($P = 0.048$);⁵⁴ the uptake of FMISO by the tumour remained relatively constant, with mean SUV_{max} values of 1.5 before and 1.4 during therapy ($P = 0.76$).⁵⁴ This pilot study involved only five patients and primarily focused on identifying correlations between the imaging metrics used and monitoring changes in the individual parameters with treatment, rather than associations between the observations and clinical treatment outcomes. However,

the pairing of parameters could be particularly useful for identifying the BTV, using FMISO-PET, and evaluating temporal response to radiotherapy, using changes in FLT and/or FDG uptake. In the context of anatomically-based planning of radiation therapy, one might expect that pretreatment regional FMISO uptake would be predictive of a limited decrease in FLT uptake from before to after treatment, reflecting the increased radioresistance of cells in hypoxic tumour regions. Further studies are required to address this hypothesis. It should also be noted that studies that incorporate multiple PET tracers at multiple time points can rapidly reach the regulatory limits on ionizing radiation and are, therefore, quite rare.

Monitoring response in clinical trials—On the basis of the evidence of improved prediction and/or monitoring of therapeutic response coming from the studies we have presented, the use of multimodality imaging in clinical trials will likely continue to expand. Owing to the considerable expenditure and technical expertise required to incorporate multimodality imaging studies into clinical trials, the imaging methods selected for a particular trial must be intimately related to the direct effects of the therapeutic intervention for which patient response is to be predicted and/or monitored. By rationally pairing quantitative imaging methods with therapeutic targets, imaging techniques can be tailored to assess and/or guide individual treatment regimens, and might, consequently, directly influence the provision of personalized medicine. The following two examples indicate how multimodality imaging studies can yield definitive recommendations on which imaging techniques should be included in prospectively planned trials.

The first example comes from a comparison of the ability of DW-MRI and FDG-PET to predict the response of locally advanced gastric adenocarcinoma to neoadjuvant therapy. In this study, Giganti *et al.*⁵⁵ assessed 17 patients using both DW-MRI and FDG-PET-CT before and after the completion of neoadjuvant therapy and found that both the post-treatment ADC and the change in ADC from baseline values (Δ ADC) were significantly inversely correlated with tumour-regression grade (TRG; $r = -0.71$, $P = 0.0011$ and $r = -0.78$, $P = 0.0002$, respectively); the mean values of Δ ADC and post-treatment ADC were also demonstrated to be significantly different ($P = 0.0009$ and $P = 0.000082$, respectively) between patients with a good response to therapy (TRG 1–3) and nonresponders (TRG 4–5).⁵⁵ However, no such correlation or significant differences were found between responders and nonresponders using the FDG-PET SUV.⁵⁵ Thus, in this setting, early data indicate that DW-MRI (as summarized by the Δ ADC) outperforms FDG-PET (as summarized by the SUV) in monitoring treatment response.

In the second study illustrating the need for appropriate, rational selection of imaging modalities for clinical trials, Galldiks *et al.*⁵⁶ assessed therapeutic response in patients with glioblastoma using MRI and O-(2-¹⁸F-fluoroethyl)-6-tyrosine (FET-PET) performed after surgery, then at early (7–10 days) and late (6–8 weeks) time points after completion of radiochemotherapy with temozolomide. FET-PET data, which can reflect an increase in the expression of amino acid transporters, was quantified—among other metrics—according to the maximum tumour-to-brain FET uptake ratio, whereas MRI was used to determine the gadolinium contrast-enhancing volume.⁵⁶ The authors reported that a decrease in the maximum tumour-to-brain FET uptake ratio of >20% between the postsurgery baseline and early postchemotherapy evaluations was predictive of progression-free survival with a

sensitivity of 83%, a specificity of 67%, and an AUC of 0.75.⁵⁶ On the other hand, changes in MRI-derived contrast-enhanced tumour volume had no significant predictive value for survival.⁵⁶

Such ‘head-to-head’ comparisons are of critical importance to determine which imaging modality (or modalities) should be included when planning prospective, early phase clinical trials. For example, selection of an inappropriate imaging modality for assessment of the specific variables that are informative of the activity of a particular treatment (such as FDG-PET in the Giganti study,⁵⁵ or DCE-MRI in the Galldiks study),⁵⁶ could potentially result in mischaracterization or complete failure to recognize clinically relevant treatment responses. In such instances, studies might have to be repeated using different imaging modalities to identify the ideal approach—in this regard, a multimodality approach could possibly reduce the number of patients (and associated cost) needed to select the appropriate imaging-based response assessment for use in future studies. The problem of identifying which imaging data should be evaluated becomes potentially even more complicated when trying to predict, rather than monitor, therapeutic response (for example, early in the course of therapy), as multiple imaging metrics—reporting on differing aspects of tumour biology—seem to simultaneously indicate both disease progression and response to treatment (Figure 3). Such multimodality and/or multiparametric imaging studies can be expensive in their own right, and require considerable development to optimize the imaging measures and their interpretation; however, this approach holds promise in enhancing the efficiency of the drug development and the clinical trial process by providing a more-complete characterization of biological changes during therapy than is usually achieved in current trials. Many technical imaging studies have been performed in the past decade, particularly with the arrival of dedicated hybrid PET-MRI scanners,^{57,58} and continued progress in this direction is needed to guide the use of imaging in clinical trials.

***In vivo* assessment of cancer biology**

Different imaging methods are typically designed for particular applications, and the utility of individual techniques is limited. Thus, one imaging modality is unlikely to sensitively and specifically characterize all relevant tumour characteristics. Furthermore, any therapeutic regimen will almost certainly affect multiple interrelated tumour characteristics (proliferation, angiogenesis, and apoptosis, for example). Therefore, the ability to measure several of these phenomena simultaneously in an individual patient can provide *in vivo* data on the relationship between them in response to a therapeutic challenge; single-modality imaging simply cannot provide such information. For instance, essentially no correlation—neither spatially within tumours, nor across patients—between FMISO and FDG uptake has been detected in either soft-tissue sarcoma or NSCLC, indicating that these methods report on fundamentally different aspects of tumour biology.^{59,60}

Using FDG and ¹⁵O-labelled water, Komar *et al.*⁶¹ demonstrated that malignant pancreatic tumours had a 60% lower blood flow, but threefold higher FDG uptake, compared with data from patients with a normal pancreas. When evaluated separately, neither blood flow nor FDG were predictors of overall survival; however, a high FDG-PET SUV-to-blood-flow ratio (that is, tumours with low blood flow but increased metabolic activity) was associated

with poorer prognosis, thereby showing the utility of combining the measures. Although these results might be expected given what is known about tumour biology (based on *ex vivo* histological data and preclinical evidence), they serve as the basis for more-advanced studies that investigate the use of these multifunctional readouts to track tumour growth and evaluate treatment response *in vivo*.

With improved characterization of the biological response of tumours to treatment, new therapeutic strategies might be developed. Kamel and co-workers⁶² used multifunctional MRI to assess early biological changes following transarterial chemoembolization (TACE) for the treatment of hepatocellular carcinoma.⁶² Specifically, DCE-MRI and DW-MRI were used to evaluate changes in tumour perfusion and cellularity, respectively, over the first month of therapy, during which no obvious changes in tumour size were observed;⁶² however, immediately after TACE, tumour perfusion was demonstrated to decrease substantially and remained low over the first 4 weeks after treatment.⁶² By contrast, the ADC increased over the 2 weeks following TACE, but then returned to pretreatment levels by 4 weeks.⁶² The initial increase in the ADC was attributed to early cellular necrosis, whereas the subsequent reduction was interpreted as the influence of tissue dehydration due to cellular necrosis. In a phase II trial of intratumoural injection of bischloroethylnitrosourea (BCNU, also known as carmustine) and radiotherapy in patients with glioma, Jenkinson *et al.*⁶³ evaluated early changes in MRI-based measures of tumour morphology, CT-based perfusion parameters, and glucose and thallium metabolism using MRI, SPECT, and CT. They observed significant decreases in tumour blood volume ($P=0.001$) and blood flow ($P<0.001$) as early as 3 days after initiation of treatment with BCNU compared with baseline values, and tumour blood volume remained decreased for nearly a month.⁶³ Histological analysis of resected tissue corroborated the imaging findings, revealing the presence of unperfused 'ghost' blood vessels within regions of tumour necrosis.⁶³ The authors hypothesized that these observations could reflect a thrombotic mechanism and the sensitivity of the tumour-associated vasculature to BCNU. A significant decrease in glucose uptake in tumours was also observed 6 days after the initiation of treatment ($P<0.001$) compared with pretreatment levels, but this effect could not be attributed to the detected vascular action of BCNU or the effects of DNA-alkylation.⁶³ These studies illustrate how multiparametric imaging can provide data that reflect not only response to treatment, but also the underlying changes in cancer biology that could potentially be exploited to optimize therapy, and underscore the potential role of imaging in the dynamic biological characterization of treatment response. Indeed, with the increased use of combined therapeutic strategies and agents targeting multiple molecular pathways, multimodality imaging could become an essential clinical tool for patient selection, treatment planning (timing), and validation of drug-target interactions. Although it is certainly true that if a multidrug regimen only targets a common pathway (for example, DNA synthesis), then one may only need a 'general' tool like FDG-PET to characterize that response. However, if the multidrug regimen consists of agents that target different pathways with different downstream manifestations, then it may be important to have methods in place that can assess these effects separately. This would be of use in, for example, determining if a patient has acquired resistance to a particular element of a multidrug regimen.

In many ways, multimodality imaging of *in vivo* tumour biology remains in its infancy but, similar to histology, this approach has the potential to transform the clinical assessment of tumours, their microenvironment, as well as the biochemical and molecular properties of the lesion. Imaging will probably serve a complementary role to traditional histology in the near future; however, for specific biological assessments (such as evaluating metabolic changes over time) and clinical scenarios (in the context of targeted treatments, for example) multifunctional imaging could become a standard-of-care option, as imaging—unlike histology—can enable noninvasive, 3D, and serial evaluations of tissue status. Nevertheless, the realization of this potentially transformative technology depends on further validation of the proposed techniques and more-efficient pathways, both federal and commercial, for clinical translation of biologically specific imaging approaches.

Barriers to adoption

From a technical perspective, quantitative multimodality imaging can be highly sensitive to variations in both hardware (data acquisition) and software (data analysis). Thus, before such approaches can be adopted in clinical trials, methods must be shown to be reproducible across multiple vendor platforms at multiple clinical sites. Furthermore, common standards must be established for reporting and interpretation of measurements. Several government–academic–industry partnerships are currently addressing this issue, including the National Cancer Institute Quantitative Imaging Network (QIN)⁶⁴ and the Radiological Society of North America Quantitative Imaging Biomarker Alliance (QIBA).⁶⁵ The QIN aims to promote research and development of methods for the measurement of tumour response to therapies in clinical trial settings using quantitative imaging, with the overall goal of facilitating clinical decision making.⁶⁴ The methods developed must be made widely available, and a major contribution of the QIBA has been the production of ‘profiles’ that provide detailed guidance on obtaining reliable and consistent quantitative imaging results across platforms, sites, and (critically) time points.⁶⁵ QIBA profiles also include information on what hardware and software features the manufacturers of imaging equipment should include in their product,⁶⁵ thereby helping to increase the practicality of performing multisite studies involving large numbers of patients. The success of partnerships such as these is critical to the acceptance of advanced imaging in clinical trials.

From a clinical perspective, much work remains to be done to associate quantitative multimodality imaging results with relevant clinical end points. As the examples cited in this article indicate, much of the current evidence for a clinical utility of multiparametric imaging stems from small studies and, therefore, requires validation in large multicentre trials. Thus, further progress in validating multimodality imaging might take advantage of multi-institution research networks, such as the Eastern Cooperative Oncology Group American College of Radiology Imaging Network (ECOG-ACRIN).⁶⁶

A key requirement is that imaging researchers work with clinicians to formulate research goals with practical relevance to medical decision making. For example, although imaging researchers might envision a future in which PET–MRI obviates the need for prostate biopsy by enabling differentiation of benign and malignant tissues, and accurate staging, more-realistic intermediate applications for PET–MRI might be in targeting prostate biopsies to

the viable neoplasm, or improving the accuracy of distinguishing extracapsular extension. These different clinical objectives need the use of different study designs and statistical methods. Furthermore, as promising as the prospect of PET–MRI might be, in general, excitement regarding this technology is tempered by both economical (such devices can cost >US\$6 million) and technical (for example, how to best use the available MRI data to perform attenuation correction of PET data) issues. As such, multidisciplinary partnerships will be of paramount importance for the appropriate development and translation of quantitative multimodality imaging methods.

In addition, gaining an understanding of the appropriate use of multimodality imaging in different contexts is an important requirement. Many of the techniques described in this article are already being actively explored by pharmaceutical companies in proof-of-concept studies of their new compounds, and for prioritizing research and development pipelines. By contrast, adoption of quantitative multimodal imaging into clinical decision making will probably move more slowly and will require a higher level of statistical qualification. Similarly, in clinical trials, quantitative multimodality imaging will continue to be used on a primarily exploratory basis until these techniques can be incorporated into standardized response-assessment strategies and accepted by regulatory bodies as valid analyses for biomarkers of drug efficacy.

Imaging and predictive oncology

Multimodality imaging can provide a wealth of data to characterize disease in individual patients. Thus, a question occurs naturally: what is the best way to synthesize this data to derive the maximum clinical utility? To date, statistical measures designed to find the largest differences between patient groups have been the point of greatest emphasis. In the future, an entire paradigm of individualized ‘predictive oncological imaging’ might arise through the use of biophysical and biomathematical models.⁶⁷

Mathematical modelling of the dynamics of tumour growth is not a novel concept; however, practical applicability of most of the current mathematical models is limited, as these models rely on data that is difficult to obtain in an intact organism with adequate spatial resolution at any given time point, let alone at multiple time points. As discussed above, multimodality imaging can provide quantitative anatomical, molecular, and functional information noninvasively, in 3D, and at multiple time points, thereby providing compelling motivation for integrating imaging data into predictive mathematical models of tumour response to therapy. Owing to the substantial heterogeneity in cancer, populating mathematical models of tumour growth and treatment response with patient-specific data is imperative. As multiple, repeat measurements are required to optimize such an approach, multimodality imaging is the most promising—if not the only—method of providing the data required. Furthermore, because the data are acquired noninvasively, the predictions derived from any model can then be directly compared with the actual clinical responses and outcomes observed in the patients in whom the images were acquired. Thus, this approach lends itself to making patient-specific predictions that can be experimentally tested.^{68–70}

After the validation of tumour-growth models that are initialized and constrained by imaging data, it could become possible to perform *in silico* experiments to select, given a set of patient-specific imaging measurements, an optimal treatment strategy. For example determining the sequence and timing of antiangiogenic and cytotoxic therapies dynamically might be important in improving the efficacy of treatment (Box 2). With a validated imaging-based model in hand, simulations could be run for each patient based on the results of multimodal imaging assessments to predict the optimal sequence, dosing, and timing of such therapies. In this way, the synthesis of imaging and modelling would truly enable the development of a field of predictive oncological imaging.

Conclusions

From a clinical perspective, enthusiasm is increasing with regard to the potential of multimodality imaging to improve our ability to accurately characterize disease and stratify patients, to assess and even predict treatment response, and to accelerate the drug development and clinical trials processes. Admittedly, current efforts in this direction have been confined to small, single-centre studies and, therefore, must be validated in larger prospective trials—but tantalizing evidence is now available to encourage the initiation of such studies. From a scientific perspective, multimodality functional imaging provides a noninvasive approach to obtain quantitative data on spatial and temporal changes in a range of biological features within tumours; these methods might provide answers to fundamental biological questions that cannot be addressed by other means. Thus, it seems highly likely that the influence of multimodality functional imaging on clinical trials and medical practice will continue to grow.

Acknowledgments

T.E.Y. thanks the National Cancer Institute for funding support through grants 1U01CA142565, 1U01CA174706, R01 CA138599, R25CA092043. R.G.A. is funded in part by the AUR GE Radiology Research Academic Fellowship. C.C.Q. thanks the Vanderbilt Ingram Cancer Center Young Ambassadors grant and NCI 1R01CA158079. The authors thank the Kleberg Foundation for generously supporting their imaging programme and NCI P30CA68485 (PI: J. Pietenpol). The authors also thank Drs J. Skinner and X. Li of the Vanderbilt University Institute of Imaging Science, Nashville, TN, USA, for preparing Figure 2 and Figure 3, respectively.

References

1. Pisano ED, et al. Diagnostic performance of digital versus film mammography for breast-cancer screening. *N Engl J Med.* 2005; 353:1773–1783. [PubMed: 16169887]
2. Carmeliet P, Jain RK. Angiogenesis in cancer and other diseases. *Nature.* 2000; 407:249–257. [PubMed: 11001068]
3. Yankeelov TE, Gore JC. Dynamic-contrast enhanced magnetic resonance imaging in oncology: theory, data acquisition, analysis, and examples. *Curr Med Imaging Rev.* 2009; 3:91–107. [PubMed: 19829742]
4. Ingrisich M, Sourbron S. Tracer-kinetic modeling of dynamic contrast-enhanced MRI and CT: a primer. *J Pharmacokinet Pharmacodyn.* 2013; 40:281–300. [PubMed: 23563847]
5. Cosgrove D, Lassau N. Imaging of perfusion using ultrasound. *Eur J Nucl Med Mol Imaging.* 2010; 37(Suppl 1):S65–S85. [PubMed: 20640418]
6. Lewis JS, Welch MJ. PET imaging of hypoxia. *Q J Nucl Med.* 2001; 45:183–188. [PubMed: 11476169]

7. Kurihara H, Honda N, Kono Y, Arai Y. Radiolabelled agents for PET imaging of tumor hypoxia. *Curr Med Chem*. 2012; 19:3282–3289. [PubMed: 22664246]
8. Yankeelov, TE.; Pickens, DR.; Price, RR., editors. Quantitative MRI of Cancer. CRC Press; 2012. p. 193-202. Series Ed. Hendee, W. R. Imaging in Medical Diagnosis and Therapy
9. He X, Yablonskiy DA. Quantitative BOLD: mapping of human cerebral deoxygenated blood volume and oxygen extraction fraction: default state. *Magn Reson Med*. 2007; 57:115–126. [PubMed: 17191227]
10. Anderson AW, et al. Effects of cell volume fraction changes on apparent diffusion in human cells. *Magn Reson Imaging*. 2000; 18:689–695. [PubMed: 10930778]
11. Tehrani OS, Shields AF. PET imaging of proliferation with pyrimidines. *J Nucl Med*. 2013; 54:903–912. [PubMed: 23674576]
12. Czernin, J. PET: Molecular Imaging and its Biological Implications. Phelps, ME., editor. Springer; New York: 2004. p. 321-388.
13. Eisenhauer EA, et al. New response evaluation criteria in solid tumours: revised RECIST guideline (version 1.1). *Eur J Cancer*. 2009; 45:228–247. [PubMed: 19097774]
14. Sundararajan L, Linden HM, Link JM, Krohn KA, Mankoff DA. 18F-Fluoroestradiol. *Semin Nucl Med*. 2007; 37:470–476. [PubMed: 17920354]
15. Meng Q, Li Z. Molecular imaging probes for diagnosis and therapy evaluation of breast cancer. *Int J Biomed Imaging*. 2013; 2013:230487. [PubMed: 23533377]
16. Treglia G, et al. The role of positron emission tomography using carbon-11 and fluorine-18 choline in tumors other than prostate cancer: a systematic review. *Ann Nucl Med*. 2012; 26:451–461. [PubMed: 22566040]
17. Kuhl DE, Hale J, Eaton WL. Transmission scanning: a useful adjunct to conventional emission scanning for accurately keying isotope deposition to radiographic anatomy. *Radiology*. 1966; 87:278–284. [PubMed: 5915433]
18. Liew SC, Hasegawa BH. Noise, resolution, and sensitivity considerations in the design of a single-slice emission-transmission computed tomographic system. *Med Phys*. 1991; 18:1002–1015. [PubMed: 1961140]
19. Lang TF, et al. Description of a prototype emission-transmission computed tomography imaging system. *J Nucl Med*. 1992; 33:1881–1887. [PubMed: 1403162]
20. Kalki K, et al. Myocardial perfusion imaging with a combined X-ray CT and SPECT system. *J Nucl Med*. 1997; 38:1535–1540. [PubMed: 9379188]
21. Beyer T, et al. A combined PET/CT scanner for clinical oncology. *J Nucl Med*. 2000; 41:1369–1379. [PubMed: 10945530]
22. Kinahan PE, Townsend DW, Beyer T, Sashin D. Attenuation correction for a combined 3D PET/CT scanner. *Med Phys*. 1998; 25:2046–2053. [PubMed: 9800714]
23. Poeppel TD, Krause BJ, Heusner TA, Boy C, Bockisch A, Antoch G. PET/CT for the staging and follow-up of patients with malignancies. *Eur J Radiol*. 2009; 70:382–392. [PubMed: 19406595]
24. Antoch G, et al. Non-small cell lung cancer: dual-modality PET/CT in preoperative staging. *Radiology*. 2003; 229:526–533. [PubMed: 14512512]
25. Lardinois D, et al. Staging of non-small-cell lung cancer with integrated positron-emission tomography and computed tomography. *N Engl J Med*. 2003; 348:2500–2507. [PubMed: 12815135]
26. Cohade C, Osman M, Leal J, Wahl RL. Direct comparison of ¹⁸F-FDG PET and PET/CT in patients with colorectal carcinoma. *J Nucl Med*. 2003; 44:1797–1803. [PubMed: 14602862]
27. Schöder H, Yeung HW, Gonen M, Kraus D, Larson SM. Head and neck cancer: clinical usefulness and accuracy of PET/CT image fusion. *Radiology*. 2004; 231:65–72. [PubMed: 14990824]
28. Pfannenbergl AC, et al. Benefit of anatomical-functional image fusion in the diagnostic work-up of neuroendocrine neoplasms. *Eur J Nucl Med Mol Imaging*. 2003; 30:835–843. [PubMed: 12682789]
29. Even-Sapir E, Keidar Z, Bar-Shalom R. Hybrid imaging (SPECT/CT and PET/CT)--improving the diagnostic accuracy of functional/metabolic and anatomic imaging. *Semin Nucl Med*. 2009; 39:264–275. [PubMed: 19497403]

30. Sauter AW, Wehrl HF, Kolb A, Judenhofer MS, Pichler BJ. Combined PET/MRI: one step further in multimodality imaging. *Trends Mol Med*. 2010; 16:508–515. [PubMed: 20851684]
31. Judenhofer MS, et al. Simultaneous PET-MRI: a new approach for functional and morphological imaging. *Nat Med*. 2008; 14:459–465. [PubMed: 18376410]
32. Yankeelov TE, et al. Simultaneous PET-MRI in oncology: a solution looking for a problem? *Magn Reson Imaging*. 2012; 30:1342–1356. [PubMed: 22795930]
33. Buchbender C, Heusner TA, Lauenstein TC, Bockisch A, Antoch G. Oncologic PET/MRI, part 1: tumors of the brain, head and neck, chest, abdomen, and pelvis. *J Nucl Med*. 2012; 53:928–938. [PubMed: 22582048]
34. Huang SH, et al. A comparative study of fused FDG PET/MRI, PET/CT, MRI, and CT imaging for assessing surrounding tissue invasion of advanced buccal squamous cell carcinoma. *Clin Nucl Med*. 2011; 36:518–525. [PubMed: 21637051]
35. Tatsumi M, et al. ¹⁸F-FDG PET/MRI fusion in characterizing pancreatic tumors: comparison to PET/CT. *Int J Clin Oncol*. 2011; 16:408–415. [PubMed: 21347626]
36. Catalano OA, et al. Clinical impact of PET/MR imaging in patients with cancer undergoing same-day PET/CT: initial experience in 134 patients—a hypothesis-generating exploratory study. *Radiology*. 2013; 269:857–869. [PubMed: 24009348]
37. Borgwardt L, et al. Increased fluorine-18 2-fluoro-2-deoxy- β -D-glucose (FDG) uptake in childhood CNS tumors is correlated with malignancy grade: a study with FDG positron emission tomography/magnetic resonance imaging coregistration and image fusion. *J Clin Oncol*. 2005; 23:3030–3037. [PubMed: 15860860]
38. Nagamachi S, et al. The usefulness of ¹⁸F-FDG PET/MRI fusion image in diagnosing pancreatic tumor: comparison with ¹⁸F-FDG PET/CT. *Ann Nucl Med*. 2013; 27:554–563. [PubMed: 23580090]
39. Pfluger T, et al. Diagnostic value of combined ¹⁸F-FDG PET/MRI for staging and restaging in paediatric oncology. *Eur J Nucl Med Mol Imaging*. 2012; 39:1745–1755. [PubMed: 22926713]
40. Walter C, et al. Clinical and diagnostic value of preoperative MR mammography and FDG-PET in suspicious breast lesions. *Eur Radiol*. 2003; 13:1651–1656. [PubMed: 12835981]
41. Zonari P, Baraldi P, Crisi G. Multimodal MRI in the characterization of glial neoplasms: the combined role of single-voxel MR spectroscopy, diffusion imaging and echo-planar perfusion imaging. *Neuroradiology*. 2007; 49:795–803. [PubMed: 17619871]
42. Yabuuchi H, et al. Parotid gland tumors: can addition of diffusion-weighted MR imaging to dynamic contrast-enhanced MR imaging improve diagnostic accuracy in characterization? *Radiology*. 2008; 249:909–916. [PubMed: 18941162]
43. Mazaheri Y, et al. Prostate cancer: identification with combined diffusion-weighted MR imaging and 3D ¹H MR spectroscopic imaging—correlation with pathologic findings. *Radiology*. 2008; 246:480–484. [PubMed: 18227542]
44. Segal E, et al. Decoding global gene expression programs in liver cancer by noninvasive imaging. *Nat Biotechnol*. 2007; 25:675–680. [PubMed: 17515910]
45. Gevaert O, et al. Non-small cell lung cancer: identifying prognostic imaging biomarkers by leveraging public gene expression microarray data—methods and preliminary results. *Radiology*. 2012; 264:387–396. [PubMed: 22723499]
46. Gutman DA, et al. MR imaging predictors of molecular profile and survival: multi-institutional study of the TCGA glioblastoma data set. 2013; 267:560–569.
47. Zinn PO, et al. Radiogenomic mapping of edema/cellular invasion MRI-phenotypes in glioblastoma multiforme. *PLoS ONE*. 2011; 6:e25451. [PubMed: 21998659]
48. Choi H. Response evaluation of gastrointestinal stromal tumors. *Oncologist*. 2008; 13(Suppl 2):4–7. [PubMed: 18434631]
49. Yanagawa M, et al. Evaluation of response to neoadjuvant chemotherapy for esophageal cancer: PET response criteria in solid tumors versus response evaluation criteria in solid tumors. *J Nucl Med*. 2012; 53:872–880. [PubMed: 22582049]
50. Teng FF, Meng X, Sun XD, Yu JM. New strategy for monitoring targeted therapy: molecular imaging. *Int J Nanomedicine*. 2013; 8:3703–3713. [PubMed: 24124361]

51. Jansen JF, et al. Tumor metabolism and perfusion in head and neck squamous cell carcinoma: pretreatment multimodality imaging with ^1H magnetic resonance spectroscopy, dynamic contrast-enhanced MRI, and [^{18}F]FDG-PET. *Int J Radiat Oncol Biol Phys.* 2012; 82:299–307. [PubMed: 21236594]
52. Thorwarth D, Eschmann SM, Holzner F, Paulsen F, Alber M. Combined uptake of [^{18}F] FDG and [^{18}F]FMISO correlates with radiation therapy outcome in head-and-neck cancer patients. *Radiother Oncol.* 2006; 80:151–156. [PubMed: 16920211]
53. Ling CC, et al. Towards multidimensional radiotherapy (MD-CRT): biological imaging and biological conformality. *Int J Radiat Oncol Biol Phys.* 2000; 47:551–560. [PubMed: 10837935]
54. Vera P, et al. Simultaneous positron emission tomography (PET) assessment of metabolism with ^{18}F -fluoro-2-deoxy-d-glucose (FDG), proliferation with ^{18}F -fluoro-thymidine (FLT), and hypoxia with ^{18}F -fluoro-misonidazole (F-MISO) before and during radiotherapy in patients with non-small-cell lung cancer (NSCLC): a pilot study. *Radiother Oncol.* 2011; 98:109–116. [PubMed: 21056487]
55. Giganti, F., et al. Response to chemotherapy in gastric adenocarcinoma with diffusion-weighted MRI and ^{18}F -FDG-PET/CT: Correlation of apparent diffusion coefficient and partial volume corrected standardized uptake value with histological tumor regression grade. *J Magn Reson Imaging.* <http://dx.doi.org/10.1002/jmri.24464>
56. Galldiks N, et al. Assessment of treatment response in patients with glioblastoma using O-(2- ^{18}F -fluoroethyl)-6-tyrosine PET in comparison to MRI. *J Nucl Med.* 2012; 53:1048–1057. [PubMed: 22645298]
57. Buchbender C, Heusner TA, Lauenstein TC, Bockisch A, Antoch G. Oncologic PET/MRI, part 1: tumors of the brain, head and neck, chest, abdomen, and pelvis. *J Nucl Med.* 2012; 53:928–938. [PubMed: 22582048]
58. Buchbender C, Heusner TA, Lauenstein TC, Bockisch A, Antoch G. Oncologic PET/MRI, part 2: bone tumors, soft-tissue tumors, melanoma, and lymphoma. *J Nucl Med.* 2012; 53:1244–1252. [PubMed: 22782313]
59. Rajendran JG, et al. [^{18}F]FMISO and [^{18}F]FDG PET imaging in soft tissue sarcomas: correlation of hypoxia, metabolism and VEGF expression. *Eur J Nucl Med Mol Imaging.* 2003; 30:695–704. [PubMed: 12632200]
60. Cherk MH, et al. Lack of correlation of hypoxic cell fraction and angiogenesis with glucose metabolic rate in non-small cell lung cancer assessed by ^{18}F -fluoromisonidazole and ^{18}F -FDG PET. *J Nucl Med.* 2006; 47:1921–1926. [PubMed: 17138734]
61. Komar G, et al. Decreased blood flow with increased metabolic activity: a novel sign of pancreatic tumor aggressiveness. *Clin Cancer Res.* 2009; 15:5511–5517. [PubMed: 19706808]
62. Kamel IR, et al. Unresectable hepatocellular carcinoma: serial early vascular and cellular changes after transarterial chemoembolization as detected with MR imaging. *Radiology.* 2009; 250:466–473. [PubMed: 19188315]
63. Jenkinson MD, et al. Phase II trial of intratumoral BCNU injection and radiotherapy on untreated adult malignant glioma. *J Neurooncol.* 2010; 99:103–113. [PubMed: 20063175]
64. Clarke LP, et al. The Quantitative Imaging Network: NCI's historical perspective and planned goals. *Transl Oncol.* 2014; 7:1–4. [PubMed: 24772201]
65. QIBA Protocols and Profiles. Radiological Society of North America. 2014. [online], <http://www.rsna.org/QIBAProtocolsandProfiles.aspx>
66. ECOG-ACRIN cancer research group. ECOG-AGRIN.org [online]. 2014. <http://ecog-acrin.org/about-us>
67. Yankeelov TE, et al. Clinically relevant modeling of tumor growth and treatment response. *Sci Transl Med.* 2013; 5:187ps9.
68. Szeto MD, et al. Quantitative metrics of net proliferation and invasion link biological aggressiveness assessed by MRI with hypoxia assessed by FMISO-PET in newly diagnosed glioblastomas. *Cancer Res.* 2009; 69:4502–4509. [PubMed: 19366800]
69. Atuegwu NC, et al. Parameterizing the logistic model of tumor growth by DW-MRI and DCE-MRI data to predict treatment response and changes in breast cancer cellularity during neoadjuvant chemotherapy. *Transl Oncol.* 2013; 6:256–264. [PubMed: 23730404]

70. Hogeia C, Davatzikos C, Biros G. An image-driven parameter estimation problem for a reaction–diffusion glioma growth model with mass effects. *J Math Biol.* 2008; 56:793–825. [PubMed: 18026731]
71. Yankeelov TE, Arlinghaus LR, Li X, Gore JC. The role of magnetic resonance imaging biomarkers in clinical trials of treatment response in cancer. *Semin Oncol.* 2011; 38:16–25. [PubMed: 21362513]
72. Thakur ML, Lentle BC. Report of a summit on molecular imaging. *J Nucl Med.* 2005; 46:11N–42N.
73. Jain R. Normalization of tumor vasculature: an emerging concept in antiangiogenic therapy. *Science.* 2005; 307:58–62. [PubMed: 15637262]
74. Batchelor TT, et al. AZD2171, a pan-VEGF receptor tyrosine kinase inhibitor, normalizes tumor vasculature and alleviates edema in glioblastoma patients. *Cancer Cell.* 2007; 11:83–95. [PubMed: 17222792]
75. Sorensen AG, et al. A “vascular normalization index” as potential mechanistic biomarker to predict survival after a single dose of cediranib in recurrent glioblastoma patients. *Cancer Res.* 2009; 69:5296–5300. [PubMed: 19549889]
76. Sorensen AG, et al. Increased survival of glioblastoma patients who respond to antiangiogenic therapy with elevated blood perfusion. *Cancer Res.* 2012; 72:402–407. [PubMed: 22127927]
77. Emblem KE, et al. Vessel architectural imaging identifies cancer patient responders to anti-angiogenic therapy. *Nat Med.* 2013; 19:1178–1183. [PubMed: 23955713]
78. Ribatti D. Vascular normalization: a real benefit? *Cancer Chemother Pharmacol.* 2011; 68:275–278. [PubMed: 21638121]
79. Vangestel C, et al. $^{99m}\text{Tc}(\text{CO})_3$ His-annexin A5 micro-SPECT demonstrates increased cell death by irinotecan during the vascular normalization window caused by bevacizumab. *J Nucl Med.* 2011; 52:1786–1794. [PubMed: 22045708]

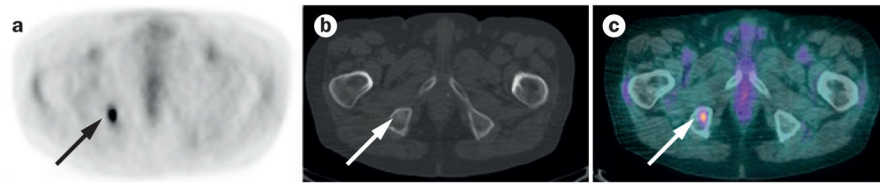


Figure 1.

Multimodality imaging in the diagnosis of metastasis in an 82-year-old woman with non-small-cell lung cancer. **a** | An axial attenuation-corrected FDG-PET image, which reveals a hypermetabolic focus in the right hemipelvis that is suggestive of a metastatic lesion, but is difficult to localize anatomically. **b** | A corresponding unenhanced axial CT image obtained using bone-window settings reveals a subtle focus of sclerosis in the right ischial tuberosity (arrow); this anomaly is difficult to identify in the absence of the PET image and cannot be definitively characterized based on the CT findings alone. **c** | A merged PET–CT image combines functional information from PET imaging with anatomical information from CT imaging, enabling conclusively definition of the lesion as a metastasis of the right ischial tuberosity. Abbreviation: FDG-PET, 2-¹⁸F-fluoro-2-deoxy-D-glucose PET.

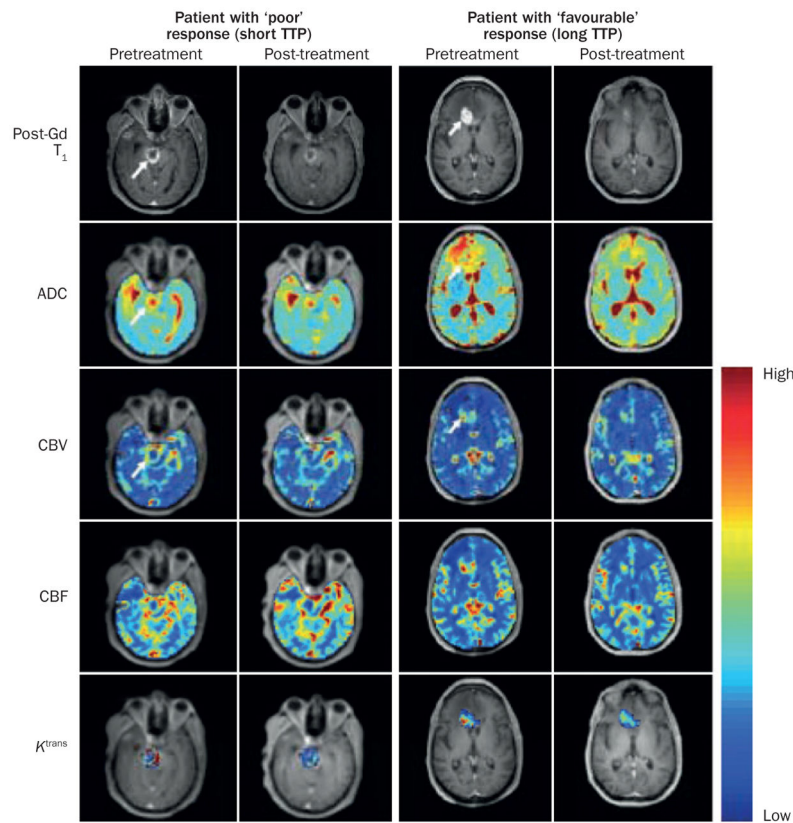


Figure 2.

A multiparametric MRI evaluation of patients with high-grade glioma before and after anti-VEGF-A antibody therapy with bevacizumab. Images from pretreatment and post-treatment MRI assessment (2 weeks after the first infusion of bevacizumab) are shown for a patient with a poor response to treatment ('short TTP'; 2.6 months) and for a patient who showed a favourable therapeutic response ('long TTP'; >9 months). The post-gadolinium contrast-enhanced T₁-weighted images (post-Gd T₁) reveal a larger decrease in the enhancing tumour volume after a single infusion of bevacizumab in the patient with a favourable response to therapy. Both patients showed a moderate (~10%) decrease in mean tumour ADC, which was probably associated with the resolution of oedema. In the patient with the favourable response mean CBV and mean CBF decreased by 44% and 55%, respectively, 2 weeks after treatment; these decreases were larger than those observed in the patient with a poor response (30% and 22%, respectively). A smaller relative change in K^{trans} was observed in the patient with the favourable response compared with patient with a poor response, although the mean baseline value of K^{trans} was considerably higher in the patient with the shorter TTP ($K^{trans}=0.278\text{min}^{-1}$) than the patient with the longer TTP ($K^{trans}=0.107\text{min}^{-1}$). Given that a tumour's cellular and vascular response to antiangiogenic therapy might not be temporally correlated and could vary dissimilarly, the serial assessment of each characteristic could prove to be highly useful in tracking and predicting therapeutic response as each metric provides a unique insight into the underlying tumour biology. Abbreviations: ADC, apparent diffusion coefficient; CBF, cerebral blood flow; CBV, cerebral blood volume; K^{trans} , volume transfer constant of contrast agent between the blood and the

extravascular extracellular space; TTP, time-to-progression; VEGF-A, vascular endothelial growth factor A.

Author Manuscript

Author Manuscript

Author Manuscript

Author Manuscript

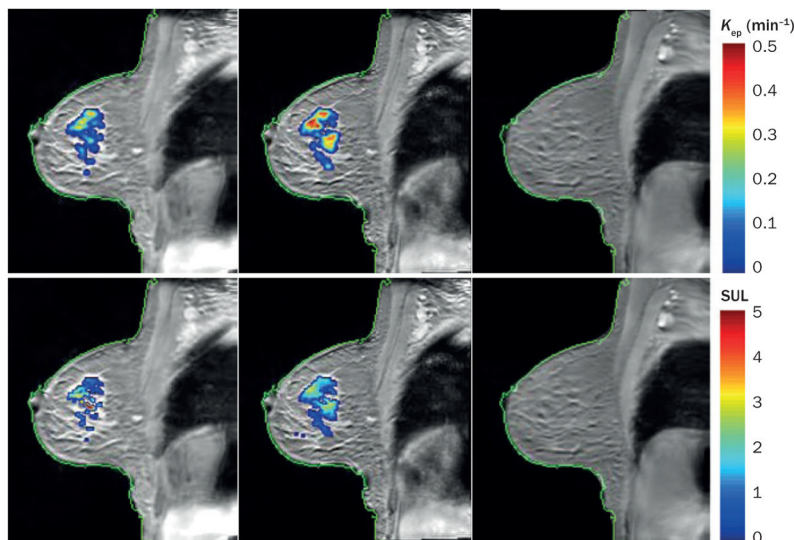


Figure 3. PET–MRI in the evaluation of treatment response in breast cancer. The top row displays k_{ep} $= (K^{trans}/v_e)$ maps overlain on a sagittal T_1 -weighted MRI of a woman with an invasive ductal carcinoma at baseline before treatment (left panel), after one cycle of neoadjuvant chemotherapy (middle panel), and at the conclusion of chemotherapy (right panel). k_{ep} represents the rate at which the contrast agent moves from the extravascular extracellular space back into the vascular space and a high k_{ep} value is indicative of malignancy. Note the increase in the number of red voxels observed after one cycle of chemotherapy (specifically, k_{ep} increased 32%, from 0.34 min^{-1} to 0.45 min^{-1}) which indicates an increase in tumour aggressiveness. Conversely, the SUL of ^{18}F -fluorodeoxyglucose during PET decreased by 30%, from 1.81 at baseline (bottom left panel) to 1.39 (bottom right panel) after one cycle of chemotherapy, indicating a possible reduction in metabolic activity; this finding argues against increased tumour aggressiveness. These apparently disparate findings indicate the potential importance of assessments that incorporate data from multimodality imaging, as well as potential complications that can arise during interpretation of such diverse parameters. That is, although such approaches can enable characterization of complementary aspects of tumour biology, substantial work is needed to determine the appropriate methods of synthesizing such data that ultimately provide the maximum benefit for patients. For this particular patient there was no residual tumour at the time of surgery (the patient achieved a pathological complete response) as seen by the images in the far right column, which were acquired within 1 week of surgery. Abbreviations: K^{trans} , volume transfer constant of contrast agent between the blood and the extravascular extracellular space; SUL, standardized uptake value normalized to lean body mass; v_e , fractional volume of the extravascular extracellular space.